

Four-states phase diagram of proteins.

OLIVIER COLLET

*équipe de Dynamique des Assemblages Membranaires,
UMR CNRS 7565, Faculté des Sciences, Université Henri Poincaré-Nancy 1,
54506 Vandoeuvre-lès-Nancy, France*

PACS. 87.14.Ee – Proteins.

PACS. 64.70-p – Specific phase transitions.

PACS. 87.15.Aa – Theory and modeling; computer simulation.

Abstract. –

A four states phase diagram for protein folding as a function of temperature and solvent quality is derived from an improved 2-d lattice model taking into account the temperature dependence of the hydrophobic effect. The phase diagram exhibits native, globule and two coil-type regions. In agreement with experiment, the model reproduces the phase transitions indicative of both warm and cold denaturations. Finally, it predicts transitions between the two coil states and a critical point.

Understanding the physical mechanism underlying protein folding remains one of the main open problems of contemporary theoretical biophysics. The interplay between protein-protein and protein-solvent interactions that drive the folding of the polypeptide may be partly investigated using full atomistic representations. Computer simulations at this level of detail are shown for instance to provide crucial information about the stability of the proteins around its native structure. Such calculations are however very time consuming and not appropriate for characterizing the large conformational space of multimeric chains, which is a crucial step toward understanding the folding problem. [1].

This has led to the emergence of alternative approaches, such as the use of simpler coarse grained models. Among these, the lattice model is probably the most popular and efficient model that allows a wide sampling of the conformational space of a given polypeptide chain [2]. Accordingly, the 16-mer placed on a two dimensional lattice has often been used to this end. [3–5] Such a chain is long enough to capture fundamental mechanism of protein folding and short enough to allow the calculation of partition function by a full enumeration in reasonable computer times.

Over a decade ago, Dinner et al. [3] used such a model to derive the three-states phase diagrams of 16 mers for different chain sequences as a function of temperature and average attraction between monomers. Coil, globule and native states were all obtained but the model failed to reproduce the well known cold denaturation. This transition, from the native to the coil state, upon lowering the temperature, consists in the loss of the order of the chain [6].

It was indeed later shown that the accuracy of the potential describing the interactions with the solvent is crucial [7]. We have recently proposed a refinement of the coupling model

that explicitly includes a temperature dependent so-called hydrophobic effect in a solvation free energy contribution [8]. This model, considering the same 16-mer chain, predicts the existence of the coil and a native states, the warm and cold denaturation transition but produces no globule states. Despite this last shortcoming the coupling models were shown to be consistent with all-atom molecular dynamics simulations of a short peptide solvated in water [9]. In the recent literature, other models dealing with the cold denaturation have also been proposed [10].

In this paper, we extend on previous calculations and propose a more comprehensive model of the hydrophobic effect that reproduces a four states phase diagram with both the warm and cold denaturation transitions. In the model, all the links between two adjacent nodes of the lattice are taken into account (see an example in fig.1). The effective hamiltonian of

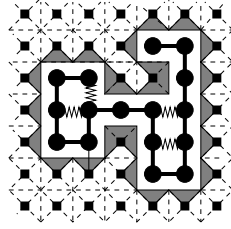


Fig. 1 – One conformation, of a 16 monomers chain (filled circles) on a two-dimensional lattice. The thick solid lines represent the covalent bonds and the springs the intrachain contacts. The solvent sites are depicted as squares each of which is divided into four solvent cells (triangles). Solvent-solvent interactions involve two adjacent solvent cells (clear triangles) whereas a solvent-monomer bond involves a monomer and a nearest solvent cell (grey triangles).

conformation m is given by:

$$\mathcal{H}_{\text{eff}}^{(m)}(T) = E_{\text{intr}}^{(m)} + F_{\text{solv}}^{(m)}(T) \quad (1)$$

The intrachain interaction energy for each conformation m is described as in Dinner et al. [3]:

$$E_{\text{intr}}^{(m)} = \sum_{i>j}^N B_{ij} \Delta_{ij}^{(m)} \quad (2)$$

where B_{ij} is the specific interaction between residue sites i and j and $\Delta_{ij}^{(m)}$ equals 1 if i and j are in contact and 0 otherwise. Monomer-monomer interactions B_{ij} are real numbers selected randomly from a normalized probability density - Gaussian distribution - with a standard deviation $\sigma = 2$. One single conformation, noted Nat, is selected at random among the more maximally compact structures, and considered as the native conformation of the sequence. Nat has 9 intrachain contacts. In the spirit of the Go-model [11], the corresponding values of interactions are described by the 9 smallest values of B_{ij} .

The free energy of solvation for each conformation may be written as a sum of two contributions:

$$F_{\text{solv}}^{(m)}(T) = \sum_{i=1}^N n_i^{(m)} f_i(T) + 2n_s^{(m)} f_s(T) \quad (3)$$

Where $n_i^{(m)}$ and $n_s^{(m)}$ are respectively the number of solvent sites surrounding residue i and the total number of solvent-solvent contacts. $f_i(T)$ is the specific free energy of a solvent cell in interaction with residue i and $f_s(T)$, that of a neat solvent cell.

Taken the extended structures (without any intrachain contacts) as the free energy reference, the effective hamiltonian may be rewritten as a summation of effective couplings between monomers (see the example of figure 2) :

$$\mathcal{H}_{\text{eff}}^{(m)}(T) = \sum_{i>j}^N B_{ij}^{\text{eff}}(T) \Delta_{ij}^{(m)} \quad \text{with} \quad B_{ij}^{\text{eff}}(T) = B_{ij} - f_i(T) - f_j(T) + 2f_s(T) \quad (4)$$

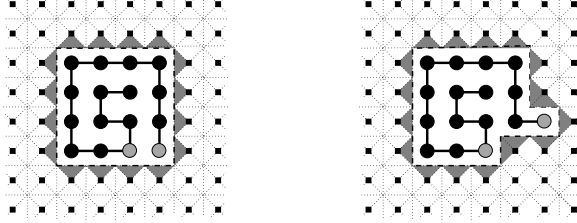


Fig. 2 – Structure *A* and *B* differs only by the contact between monomers 5 and 16. The effective couplings between these monomers is simply the effective hamiltonian difference between conformations *A* and *B*, calculated by a counting of the lattice links : $B_{5,16}^{\text{eff}} = B_{5,16} - f_5(T) - f_{16}(T) + 2f_s(B_s, T)$

Recently, Silverstein *et al.* [12] gave a description of the hydrophobic effect in terms of two energy spectra that best fits their simulation data. These results exhibits a low degenerated, narrow, (respectively high degenerated, extended,) spectra for neat water (respectively for aqueous solution with a non polar solute). Here, this physical picture is reduced further. The energy spectra of the solvent in interaction with monomer *i* consists of N_s energy values $B_i^{(j)}$, ($j = 1, N_s$) selected from a Gaussian distribution with standard deviation σ , while the energy spectrum of the neat solvent is given by a unique level, N_s^α -fold degenerated, of energy B_s . Small values of B_s models bad solvent and large values good solvent. Extending on our previous model, [8] we introduce here an extra parameter α , representing the degeneracy ratio between the bulk and the first shell solvent cells. As the total degeneracy of the latter is higher than that of the former [12], one has $\alpha < 1$ and these degeneracies being related to the number of solvent configurations N_s is a large number.

Accordingly, the free energies associated with the neat solvent and that of solvation of each monomer *i* are respectively given by :

$$f_s(B_s, T) = B_s - \alpha T \ln N_s \quad (5)$$

$$f_i(T) = -T \ln z_i(T) \quad (6)$$

where $z_i(T)$ is the partition function of the solvent around monomer *i*. For large values of N_s , it may be written using a continuous formalism as :

$$z_i(T) = N_s \int_{B_i^{\min}}^{\infty} n(B_i) \exp\left(-\frac{B_i}{T}\right) dB_i \quad (7)$$

where $n(B_i)$ is the normalized Gaussian distribution truncated at $B_i^{\min} = \min_j B_i^{(j)}$, specific to each residue:

$$n(B_i) = \begin{cases} 0 & \text{if } B < B_i^{\min} \\ \frac{\exp\left(-\frac{B_i^2}{2\sigma^2}\right)}{\frac{\sigma}{2}\sqrt{2\pi} \operatorname{erfc}\left(\frac{B_i^{\min}}{\sigma\sqrt{2}}\right)} & \text{if } B \geq B_i^{\min} \end{cases} \quad (8)$$

Equation (6) may therefore be rewritten as:

$$z_i(T) = N_s \exp\left(\frac{\sigma^2}{2T^2}\right) \frac{\operatorname{erfc}\left(\frac{B_i^{\min}}{\sigma\sqrt{2}} + \frac{\sigma\sqrt{2}}{2T}\right)}{\operatorname{erfc}\left(\frac{B_i^{\min}}{\sigma\sqrt{2}}\right)} \quad (9)$$

The density of probability that the smallest value of the N_s set, chosen at random with a Gaussian distribution, be B^{\min} , is :

$$\mathcal{G}_{N_s}(B^{\min}) = N_s g(B^{\min}) \mathcal{P}(x \geq B^{\min})^{N_s-1} \quad (10)$$

where $g(B^{\min})$ is the density of probability to select B^{\min} and $\mathcal{P}(x \geq B^{\min})$ the probability to draw a value x larger than B . Thus, for each residue i , B_i^{\min} is selected from the probability density:

$$\mathcal{G}_{N_s}(B) = \frac{N_s}{\sigma\sqrt{2\pi}} \exp\left(-\frac{B^2}{2\sigma^2}\right) \left(\frac{1}{2} \operatorname{erfc}\left(\frac{B}{\sigma\sqrt{2}}\right)\right)^{N_s-1} \quad (11)$$

The state of the chain under each set of conditions is determined from statistical equilibrium averages. For an observable $X^{(m)}$, the average over peptide structures may be defined as:

$$\langle X(B_s, T) \rangle = \sum_{m=1}^{\Omega} X^{(m)} P_{eq}^{(m)}(B_s, T) \quad (12)$$

with

$$P_{eq}(B_s, T) = \frac{\exp\left(-\frac{\mathcal{H}_{eff}^{(m)}}{T}\right)}{\sum_{m=1}^{\Omega} \exp\left(-\frac{\mathcal{H}_{eff}^{(m)}}{T}\right)} \quad (13)$$

This expression allows the estimate of the chain entropy, $S_{ch}(B_s, T) = -\langle \ln P_{eq} \rangle$, the compactness of the peptide, defined as the average of $N_c^{(m)} = \frac{1}{9} \sum_{i>j}^N \Delta_{ij}^{(m)}$ where $\sum_{i>j}^N \Delta_{ij}^{(m)}$ is the number of intra-chain contacts of structure m , and the order of the peptide, defined as the average of $Q^{(m)}$, the pairwise contact overlap of the structures with the native conformation ($Q^{(m)} = \frac{1}{9} \cdot \sum_{i>j}^N \Delta_{ij}^{(m)} \Delta_{ij}^{\text{Nat}}$). The number of contacts of the more maximally compact structures (i.e. 9 for the specific chain length studied here), appears in the two above averages in order to normalized them to 1.

For a 16-mer chain model on a two dimensional lattice, the total number of structures is $n_{\text{tot}} = 802075$ among which $n_{\text{ext}} = 116579$ have zero contact. For given values of B_s and T , the point state in the phase diagram is determined by $\langle Q \rangle$, $\langle N_c \rangle$ and S_{ch} . When $\langle Q \rangle > 0.66$, the peptide is considered in the Native phase. When $\langle Q \rangle < 0.66$ and $\langle N_c \rangle > 0.66$, only some compact structures are relevant, and the chain is in the so-called globule state. When $\langle N_c \rangle < 0.66$ and $S_{ch} = \ln n_{\text{ext}}$, the peptide is mainly in the extended conformation and the phase is coil type II. Last, when $\langle N_c \rangle < 0.66$ and $S_{ch} > \ln n_{\text{ext}}$, almost all chain structures have a non zero probability to occur. This state is referred to as coil-type I.

By setting the model parameters to $\sigma = 0$ and $\alpha = 1$, the temperature dependence of the hydrophobic effect is effectively removed. Under such conditions, the corresponding phase diagrams is similar to that determined by Dinner et al. [3]. On the other hand, the two states phase diagram where the warm and cold denaturation are present [8] may be obtained by setting $\sigma = 2$, $\alpha = 0.5$ and $N_s = 10^5$.

For discussing the four state phase diagram, we set, in the following, the model parameters to $\sigma = 2$, $\alpha = 0.9$ and $N_s = 10^5$. The results are mildly sequence dependant. We therefore

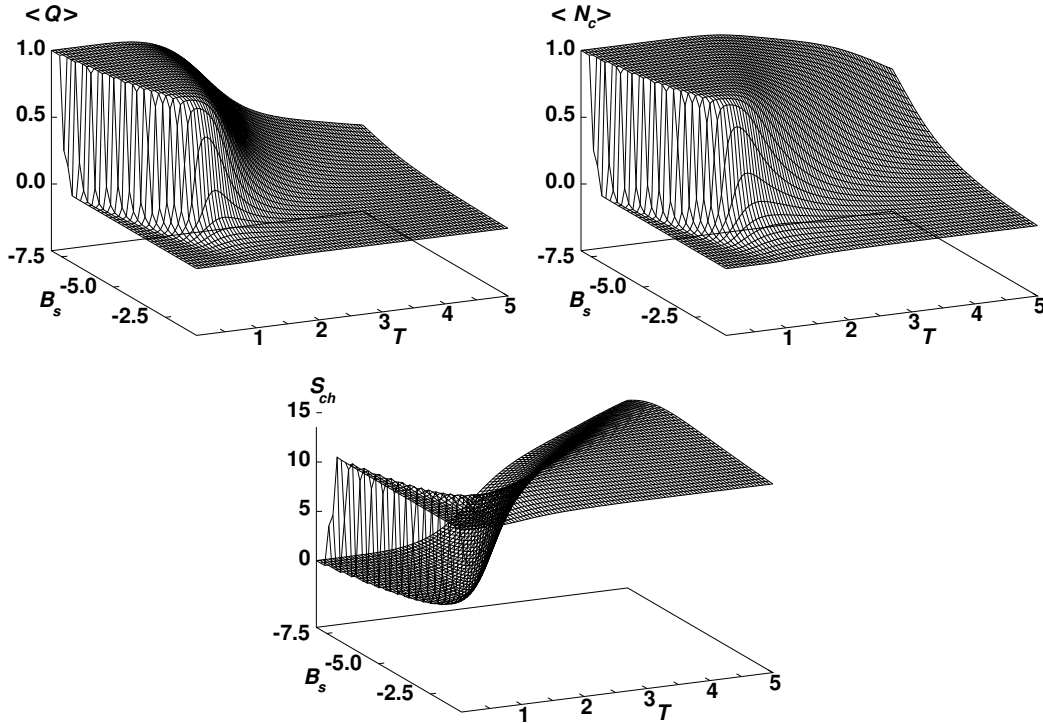


Fig. 3 – Averages of the order parameter $\langle Q \rangle$, the compactness $\langle N_c \rangle$ and the chain entropy S_{ch} as functions of B_s and T .

select a particular sequence, and investigate its corresponding phase behavior. $\langle N_c \rangle$, $\langle Q \rangle$ and S_{ch} are displayed in fig.3 as a function of B_s and T . Several qualitative features are directly observed from the 3-d plots. These may be classified depending on B_s as follow:

For $B_s < -7.5$, the $\langle Q \rangle$ plots indicate that the peptide is in the native phase at low temperature and in denatured phase at high temperature. Depending on the B_s value, the transitions in $\langle Q \rangle$ and $\langle N_c \rangle$ take place at different temperatures, noted hereafter T_w and T_{ex} respectively (i.e. $\langle Q \rangle(B_s, T_w(B_s)) = 0.66$ and $\langle N_c \rangle(B_s, T_{ex}(B_s)) = 0.66$). As for $T > T_{ex}$, the chain entropy becomes an increasing function of temperature (up to $\ln n_{tot}$), one may identify three regions corresponding to the following phases: a coil type I phase for temperatures above T_{ex} , a globule phase between T_w and T_{ex} , and a native state below T_w .

For $-7.5 < B_s < -2.5$, in addition to the states described above, transitions toward denatured states ($\langle Q \rangle \rightarrow 0$) take place at low temperatures. Such transitions, occurring at temperatures T_c that depend on B_s , represent cold denaturation. Below T_c , the chain entropy is constant and equals $\ln n_{ext}$ which indicates that the low temperature region corresponds to the coil type II state.

For B_s values above -2.5, $\langle Q \rangle$, $\langle N_c \rangle$ are very small. The chain is always in a coil state, regardless of the temperature. These values of B_s are therefore indicative of good solvation. Different states are however observed as shown from the $\langle N_c \rangle$ and S_{ch} plots (fig.4). At low temperature, the compactness is rigourously null and the chain entropy equals $\ln n_{ext}$, indicating that the peptide is in coil type II state. As the temperature increases, so does the entropy until reaching $\ln n_{tot}$ and the chain is in coil type I phase. To better delineate the

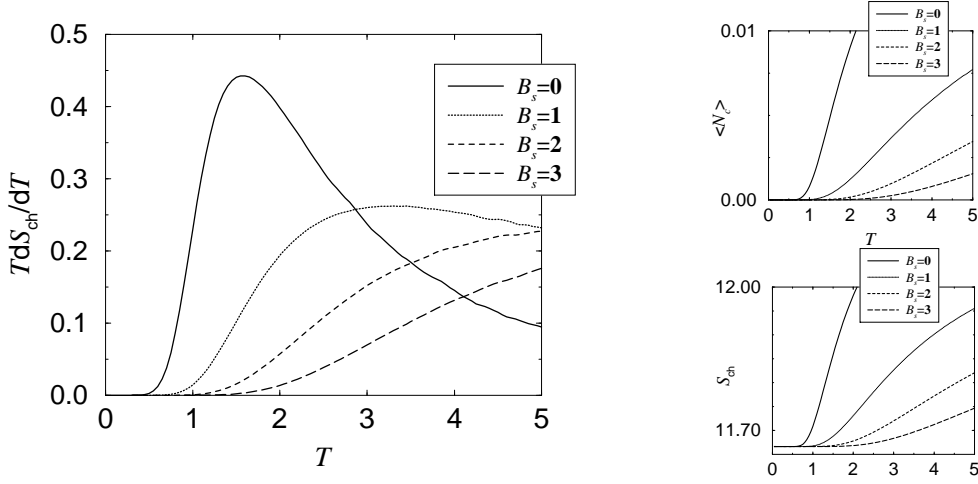


Fig. 4 – Statistical averages of the chain in interaction with good solvents modelled by $B_s = \{0, 1, 2, 3\}$ versus T . Top-left: chain entropy. Top-right: compactness. Bottom: heat capacity.

frontier between the coil type I and coil type II regions, we have estimated numerically $T \frac{dS_{ch}}{dT}$, the contribution of the chain to the heat capacity of the system as a function of temperature. For $B_s < 2.0$, these contributions undergo a maxima at $T = T_d$, which is a signature of a first order disordered-disordered transition between the two coil phases. For $B_s > 2.0$, the peak is no longer observed.

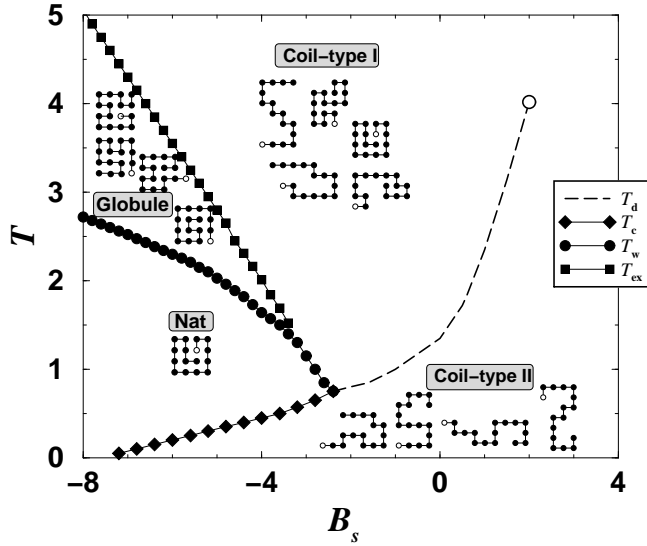


Fig. 5 – Phase diagram of the chain as a function of the solvent quality and the temperature. All the structures are observed in the coil type I, only the extended ones in the coil type II, only the compact ones in the globule and the sole native conformation in the nat region.

The previous results are summarized in the phase diagram reported in fig.5. For the particular sequence considered here, four states are distinguished. The native, globule and coil-type I phases coexist at the triple point: $(B_s, T) = (-3.4, 1.40)$ and the native, coil-type

I and coil-type II phases coexist at $(B_s, T) = (-2.4, 0.72)$. A critical point is observed at $(B_s, T)_c = (2.0, 4.0)$. Thus, moving along the B_s and T axes, transitions from Coil Type I and Coil Type II without crossing any peak in the heat capacity are allowed. Very small and smooth variations in S_{ch} , $\langle Q \rangle$ and $\langle N_c \rangle$ occur on these ways. This confirms that Coil Type I and Coil Type II are two phases of the extended state, which implies that warm and cold denaturations are, indeed, transitions toward the same extended state. The existence of a hypothetical supercritical phase for $B_s > 2.0$ or $T > 4.0$ is not clear. The nature of the set of structures relevant in such an speculative region should be investigated by the detailed study of effective hamiltonian spectra as function of the temperature.

Last, in the simulations performed with $\alpha = 0.5$ [8], the Globule and Coil Type I phases disappear leaving only the warm and the cold transitions between Coil Type II and Nat.

In summary, we have shown that the suitable solvation model presented in this paper allows to calculate, for the first time, a four-state phase diagram of a peptide chain. One would need, however, to elucidate the physical meaning of all the model parameters N_s , σ and α and their relative values for the 20 natural amino acids for a complete understanding of the mechanism responsible for protein folding. Last, it must be understood that similar phase diagrams are obtained if the same value of B_i^{\min} is affected to every residue. However, we choose to select one value of B_i^{\min} for each residue in order to model the specificity of the hydrophobicity of each monomer of the protein.

* * *

It is a pleasure to acknowledge Mounir Tarek for helpful discussions and critical reading of the manuscript.

REFERENCES

- [1] KARPLUS M. and SHAKHNOVICH E., *Theoretical Studies of Thermodynamics and Dynamics*, edited by CREIGHTON, T. E. (W. H. Freeman and Company) 1992, p. 127-193 ; DUAN Y. and KOLLMAN P., *Science*, **282** (1998) 740 ; SNOW C. NGUYEN H. PANDE V. and GRUEBELE M., *Nature*, **420** (2002) 102
- [2] SHAKHNOVICH E. I. and GUTIN A. M., *Nature*, **346** (1990) 773 ; LAU K. F. and DILL K. A., *Macromolecules*, **22** (1989) 3986 ; CHAN H. S. and DILL K. A., *J. Chem. Phys.*, **92** (1990) 3118 ; SHAKHNOVICH E. I., *Phys. Rev. Lett.*, **72** (1994) 3907 ; BRYNGELSON J. D. ONUCHIC J. N. SOCCI N. D. and WOLYNES P. G., *Proteins Struct. Funct. Genet.*, **21** (1995) 167
- [3] DINNER A. ŠALI A. KARPLUS M. and SHAKHNOVICH E., *J. Chem. Phys.*, **101** (1994) 1444
- [4] CIEPLAK M. AND VISHVESHVARA S. and BANAVAR J. R., *Phys. Rev. Lett.*, **77** (1996) 3681
- [5] COLLET O., *Phys. Rev. E*, **67** (2003) 061912
- [6] PRIVALOV P. L., *Crit. Rev. Biochem. Mol. Biol.*, **25** (1990) 281
- [7] BRYNGELSON J.D., *J. Chem. Phys.*, **100** (1994) 6038
- [8] COLLET O., *Europhys. Letters*, **53** (2001) 93
- [9] COLLET O. AND CHIPOT C., *J. Am. Chem. Soc.*, **125** (2003) 6573
- [10] DE LOS RIOS P. and CALDARELLI G., *Phys. Rev. E*, **62** (2000) 8449 ; BAKK A., HOYE J. and HANSEN A., *Biophysical Journal*, **82** (2002) 713
- [11] GO N. and ABE H., *Biopolymers*, **20** (1981) 1013
- [12] SILVERSTEIN K.A.T., HAYMET A.D. and DILL K.A., *J. Chem. Phys.*, **111** (1999) 8000

0.020

0.015

0.010

0.005

0.000

